Quality by Design-Based Crystallization of Curcumin Using Liquid Antisolvent Precipitation: Micromeritic, Biopharmaceutical, and Stability Aspects

Sananda Som,[1] Sachin Kumar Singh,[1] Gopal L. Khatik,[1] Bhupinder Kapoor,[1] Monica Gulati,[1] Gowthamarajan Kuppusamy,[2] Nandha Kumar Anandhakrishnan,[2] Bimlesh Kumar,[1] Ankit Kumar Yadav,[1] Rajesh Kumar,[1] Pankaj Kumar Singh,[3] Rubiya Khursheed,[1] Rajan Kumar,[1] Narendra Kumar Pandey,[1] Jivan Jyoti,[1] Souvik Mohanta,[1] and Omji Porwal[4]

[1]*School of Pharmaceutical Sciences, Lovely Professional University, Phagwara, India.*
[2]*Department of Pharmaceutics, JSS College of Pharmacy, JSS Academy of Higher Education and Research (Deemed to be University), Ootacamund, Tamilnadu.*
[3]*Department of Pharmaceutics, National Institute of Pharmaceutical Education and Research, Hyderabad, India.*
[4]*Department of Pharmacognosy, Faculty of Pharmacy, Ishik University, Kurdistan, Iraq.*

ABSTRACT

The aim of present study was to introduce the role of quality by design to produce curcumin crystals with enhanced dissolution rate and bioavailability. The liquid antisolvent method was used to produce crystals. The crystal growth was controlled using the Box–Behnken design. The variables used in the crystallization process included the ratio of pyrocatechol to polyethylene glycol (PEG) 1500, solvent addition rate, stirring time, and stirring speed. Combination of these variables was found to yield curcumin crystals of 2.45 ± 0.56 μm size and 0.321 polydispersity index that exhibited enhanced solubility, dissolution rate, product yield, and compressibility. The optimized curcumin crystals were characterized by Fourier-transform infrared spectrophotometer (FT-IR), nuclear magnetic resonance, differential scanning calorimetry, X-ray powder diffraction, and scanning electron microscopy. The dissolution rate and oral bioavailability of optimized curcumin crystals were found to be 2.66- and 7.08-folds higher than its unprocessed form. The optimized crystals were found stable for 6 months under accelerated temperature of 40°C and 75% relative humidity as there was no significant difference observed in the crystal size and dissolution profile.

Keywords: polymorph, Box–Behnken design, dissolution, bioavailability, crystallization

INTRODUCTION

Poor solubility of drugs poses a notable challenge in the development of new products leading to low and erratic bioavailability, resulting in both safety and efficacy concerns, particularly in case of oral administration.[1] Although numerous technologies exist for enhancing the bioavailability of drugs with low solubility, the success of these approaches greatly depends on the physical and chemical nature of the molecules being developed and a universal applicability of any approach has not yet been achieved.[1,2] Crystal engineering of drug substances provides a unique approach for improvement of physicochemical as well as biopharmaceutical properties such as solubility, bioavailability, absorption, metabolism, systematic elimination, stability, decomposition, and dissolution rate.[1] The approach is a combination of both crystal engineering and supramolecular chemistry, which allows researchers to design products with the desired physicochemical parameters.[3] This may be done by varying various intermolecular interactions, including hydrogen bonding and noncovalent interactions such as halogen bond, π-π, and columbic interaction. The desired characteristics can be achieved without altering the chemical composition of the active pharmaceutical ingredient (API).

A number of methods are reported to generate crystals of APIs such as the antisolvent addition method, supersaturation, additive mediated method, and grinding.[4] Among them, the antisolvent addition is the most preferred method for

controlling the growth of crystals at the laboratory as well as industrial scale.[4] The crystal formation takes place in three different steps, competitive nucleation, crystal growth, and transformation from metastable to stable forms. Hence, the operational conditions that affect any of the abovementioned steps assume high significance. In antisolvent-mediated crystallization, the solvent to antisolvent ratio, stirring rate of reactant solutions, time of mixing, and antisolvent addition rate are considered the primary influencing factors, while addition of additives and modulation of pH are the secondary influencing factors.[4,5] In the present study, these factors were evaluated for their effect on crystal growth and aqueous solubility of obtained crystals. The crystallization process was operated through quality by design (QbD) approach. QbD approach involves systematic and multivariate experiments that are not possible with traditional approaches. It is based on the principles of design of experiments that help in risk evaluation of the quality risk management process.[6] In the present study, the crystallization process was operated through Box–Behnken design (BBD), in which the influence of various processing factors on response was recorded to generate a particular type of polymorph with desired pharmaceutical and biopharmaceutical properties. BBD is a type of fractional factorial design that helps in optimization of independent variables with lesser number of experiments.

Curcumin (CUR), a hydrophobic phenol having the chemical name (1E,4Z,6E)-5-hydroxy-1,7-bis(4-hydroxy-3-methoxyphenyl)-hepta-1,4,6-trien-3-one, is the principal curcuminoid obtained from the rhizomes of herb *Curcuma longa*.[7] CUR is widely reported for its antioxidant, anti-inflammatory, anticancer, and antidiabetic effects.[8] Despite this, much of its therapeutic potential lies unexplored due to its poor aqueous solubility and thus poor bioavailability.[9]

In the present study, liquid antisolvent precipitation (LAP) was designed through BBD, in which the influence of various processing factors on response was recorded to generate CUR crystals with improved dissolution rate and oral bioavailability. The optimized crystals were characterized through various analytical techniques such as diffraction scanning calorimetry (DSC), powder X-ray diffraction (PXRD) studies, scanning electron microscopy (SEM), Fourier-transform infrared spectrophotometer (FT-IR), and Fourier transform proton nuclear magnetic resonance (FT-^{1}HNMR), as well as micromeritic techniques such as angle of repose, bulk density (BD), tapped density (TD), Carr's index, and Hausner ratio (HR). In addition to this, the tablets of these crystals were prepared to understand the effect of crystal structure and shape on tablet hardness, friability, disintegration, and dissolution. The prepared tablets of CUR crystals were subjected to pharmacokinetic studies and the oral bioavailability thereof was compared with that of its existing unprocessed form.

EXPERIMENTAL

Materials

CUR, stearic acid, malonic acid, beta cyclodextrin (β-CD), and oxalic acid were purchased from Central Drug House (CDH) Pvt. Ltd. (Delhi, India). Tartaric acid, succinic acid (SA), maleic acid, pyrocatechol, polyethylene glycol (PEG) 1500, and ethanol were purchased from BB Chemicals Pvt. Ltd. (Amritsar, India). Salicylic acid and gallic acid were purchased from Loba Chemie Pvt. Ltd. (Mumbai, India). Benzoic acid was purchased from Hi-Media Laboratory Pvt. Ltd. (Mumbai, India). All other reagents were of analytical grade. Triple distilled water was used for the entire study.

Preparation of CUR Crystals Using Additive-Mediated LAP

To carry out this process, various additives, that is, gallic acid, malonic acid, stearic acid, benzoic acid, salicylic acid, oxalic acid, maleic acid, SA, L-tartaric acid, and pyrocatechol and PEG 1500 in the molar ratio 1:1 with the drug were screened. Apart from these, binary mixtures, ternary mixtures, that is, CUR:SA:β-CD in 1:1:1 were also used. The details of binary and ternary mixtures are shown in *Table 1*. These binary and ternary mixtures were weighed accurately and dissolved in 60 mL of ethanol. Water (200 mL) was used as antisolvent because CUR is practically insoluble in water. The drug-excipient solution was filled in a glass burette, while water (200 mL) was kept in a 500 mL glass beaker placed on a magnetic stirrer (2MLH; REMI) at a stirring speed of 2,000 rpm. Once the assembly was set and calibrated, the drug-excipient solution was added to water at a flow rate of 1 mL/min. After complete addition of solvent to water, stirring was continued for 1 h. The dispersion containing crystals was filtered through Whatman No. 1 filter paper. The obtained crystals were dried in a hot air oven (C1280; Cadmach Machineries, New Delhi, India) at 40°C for 1 h to remove any residual solvent/water present in it. Percentage yield was calculated. The dried crystals were subjected to solubility studies.

From this initial study, it was observed that the solubility of CUR crystals prepared by the antisolvent method using a binary mixture of pyrocatechol and CUR as well as a binary mixture of PEG 1500 and CUR in 1:1 ratio showed maximum solubility. Hence, these two excipients were further explored.

Design of Experiment

Initial screening trials were carried out by varying the solvent to antisolvent ratio, stirring rate, solvent addition rate, and stirring. Results from the initial screening trials suggested

Table 1. Solubility Studies and Percentage Yield of Prepared Crystal from Antisolvent Addition Method

Batch No.	Crystals	Amount taken (g)	% Solubility	% Yield
B1	CUR+gallic acid	0.2 + 0.09	7.33 ± 0.11	80 ± 2.33
B2	CUR+malonic acid	0.2 + 0.05	7.14 ± 0.10	70 ± 1.45
B3	CUR+stearic acid	0.2 + 0.1	9.16 ± 1.10	84 ± 3.65
B4	CUR+benzoic acid	0.2 + 0.065	8.04 ± 1.01	85 ± 1.76
B5	CUR+salicylic acid	0.2 + 0.074	7.12 ± 2.00	78 ± 2.45
B6	CUR+oxalic acid	0.2 + 0.048	8.01 ± 2.01	80 ± 3.76
B7	CUR+maleic acid	0.2 + 0.0724	8.02 ± 3.01	76 ± 1.87
B8	CUR+L-tartaric acid	0.2 + 0.081	9.12 ± 3.11	72 ± 2.87
B9	CUR+succinic acid	0.2 + 0.068	8.33 ± 3.10	89 ± 4.10
B10	CUR+succinic acid+beta cyclodextrin	0.2 + 0.068 + 0.6	10.99 ± 7.11	80 ± 3.09
B11	CUR+pyrocatechol	0.2 + 0.12	15.55 ± 5.12	89 ± 2.77
B12	CUR+PEG 1500	0.2 + 0.81	11.45 ± 4.13	87 ± 3.19

CUR, curcumin; PEG, polyethylene glycol.

that antisolvent ratio did not affect the solubility of formed crystal, however, pyrocatechol to PEG ratio (X_1), speed of stirring (X_2), time of stirring (X_3), and solvent addition rate (X_4) were the main factors that significantly affected solubility. Hence, these parameters were further explored to see the significant effect at three levels of −1, 0, and +1 (*Table 2*), which affected the responses, that is, % solubility (Y_1), percentage drug release at 120 min (Q_{120}%, Y_2), % yield (Y_3), and particle size (Y_4).

A set of 29 experiments (*Table 2*) using BBD was adopted. Different batches were prepared according to the obtained runs. The obtained values for the responses were supported by linear functions of independent variables (please refer to the Results and Discussion section). For an approximation of the function, first-order polynomial was used for linear models [Eq. (1)]:

$$Y = \beta_0 + \beta_1 X_1 + \beta_2 X_2 + \beta_3 X_3 + \beta_4 X_4 + \text{experimental error} \quad (1)$$

In the above equation, Y represents the responses, X represents independent variables, and β represents the coefficients.

Characterization of Developed Crystals

Solubility studies. Unprocessed CUR (10 mg) was taken in a 50 mL standard volumetric flask and 10 mL of water was added to this. The dispersion was kept on a mechanical shaker for 24 h at room temperature and shaken at 100 rpm. After 24 h, the flask was taken off from the shaker and kept aside for 1 h to sediment the undissolved CUR. The supernatant was taken and filtered through a 0.45 μm membrane filter and the clear filtrate was collected. Suitable dilutions of supernatant were prepared and the absorbance values of the diluted filtrate were recorded at 420 nm using a double beam ultraviolet visible spectrophotometer (Shimadzu, Model: UV-1800). Similarly, for the optimized CUR crystals, an amount equivalent to 10 mg of CUR was taken separately in a 50 mL standard volumetric flask from all the prepared batches and dispersed in 10 mL of water. The procedure was carried out as reported for unprocessed CUR and suitable dilutions were prepared. The absorbance of prepared dilutions was recorded at 420 nm. The calibration curve was prepared and it was found linear in the range of 2–12 μg/mL as the coefficient of regression (R^2) was found to be 0.999. The regression equation obtained was $y = 0.238x + 0.0603$. The amount of drug solubilized was calculated using the calibration curve method. Percentage solubility was calculated as per formula given in Equation (2):

$$\%\ Solubility = Amount\ of\ drug\ solubilized \div Total\ amount\ of\ drug\ added\ in\ solvent \times 100 \quad (2)$$

Calculation of percentage yield. The percentage yield was calculated by dividing actual yield of optimized CUR crystals by the theoretical yield and multiplying the obtained value by 100. The theoretical yield is the maximum amount of product that can be produced in a reaction. The formula to calculate percentage yield is given in Equation (3):

$$\%\ \text{Yield} = \frac{Actual\ yield}{\text{Theoritical yield}} \times 100 \quad (3)$$

Size analysis of optimized CUR crystals. The dried optimized CUR crystals (5 mg) were reconstituted in 100 mL double-distilled water and analyzed for particle size and size distribution using Beckman Coulter LS 13320. The readings were recorded in triplicate and the results were recorded as average of these readings.

Table 2. Factor Level and Response Data for Box–Behnken Design

Run	Factor 1, catechol to PEG ratio, mg (X_1)	Factor 2, speed of stirring, rpm (X_2)	Factor 3, time of stirring, min (X_3)	Factor 4, feed rate, mL/min (X_4)	Response 1, solubility, % (Y_1)	Response 2, Q_{120}, % (Y_2)	Response 3, yield, % (Y_3)	Response 4, particle size D90, μm (Y_4)
1	0.25 (–1)	1,500 (0)	75 (0)	0.3 (+1)	29.88	37.45	20	2.22
2	0.46 (0)	1,500 (0)	75 (0)	0.23 (0)	25.6	46.64	40	3.45
3	0.46 (0)	1,800 (+1)	90 (+1)	0.23 (0)	32.3	64.49	60	1.98
4	0.46 (0)	1,200 (–1)	75 (0)	0.15 (–1)	19.39	22.71	60	4.12
5	0.46 (0)	1,500 (0)	75 (0)	0.23 (0)	28.67	31.84	100	3.89
6	0.46 (0)	1,500 (0)	90 (+1)	0.15 (–1)	56.98	78.95	100	2.57
7	0.25 (–1)	1,500 (0)	75 (0)	0.15 (–1)	23.46	46.24	40	4
8	0.46 (0)	1,500 (0)	90 (+1)	0.3 (+1)	33.79	47.14	60	3.0
9	0.66 (+1)	1,800 (+1)	75 (0)	0.23 (0)	55.04	86.64	98	2.22
10	0.46 (0)	1,500 (0)	60 (–1)	0.3 (+1)	29.6	38.91	60	2.67
11	0.66 (+1)	1,500 (0)	75 (0)	0.15 (–1)	55.95	96.27	100	1.22
12	0.46 (0)	1,500 (0)	75 (0)	0.23 (0)	56.89	78.95	40	3.28
13	0.46 (0)	1,500 (0)	60 (–1)	0.15 (–1)	24.02	46.92	40	2.89
14	0.46 (0)	1,500 (0)	75 (0)	0.23 (0)	51.11	100	100	4.16
15	0.66 (0)	1,200 (–1)	75 (0)	0.23 (0)	46.44	92.79	93	4.21
16	0.66 (0)	1,500 (0)	90 (+1)	0.23 (0)	52.53	89.29	97	2.91
17	0.25 (–1)	1,200 (–1)	75 (0)	0.23 (0)	28.77	39.19	40	2.58
18	0.46 (0)	1,200 (–1)	75 (0)	0.3 (+1)	21.32	29.08	40	4.97
19	0.66 (+1)	1,500 (0)	60 (–1)	0.23 (0)	46.16	86.74	88	3.56
20	0.46 (0)	1,500 (0)	75 (0)	0.23 (0)	56.89	78.95	60	3
21	0.25 (–1)	1,500 (0)	60 (–1)	0.23 (0)	37.43	69.02	80	3.98
22	0.46 (0)	1,800 (+1)	60 (–1)	0.23 (0)	29.7	47.57	60	1.62
23	0.46 (0)	1,800 (+1)	75 (0)	0.3 (+1)	34.35	63.33	100	1.87
24	0.25 (–1)	1,500 (0)	90 (+1)	0.23 (0)	26.89	78.95	55	2.68
25	0.66 (+1)	1,500 (0)	75 (0)	0.3 (+1)	53.92	86.64	95	4.2
26	0.46 (0)	1,200 (–1)	60 (–1)	0.23 (0)	50.27	78.92	40	5.12
27	0.25 (–1)	1,800 (+1)	75 (0)	0.23 (0)	20.94	26.77	60	4.19
28	0.46 (0)	1,200 (–1)	90 (+1)	0.23 (0)	30.63	46.92	40	8.61
29	0.46 (0)	1,800 (+1)	75 (0)	0.15 (–1)	56.89	78.95	20	2.18

Micromeritic studies. The optimized batch of CUR crystals was subjected to micromeritic studies such as angle of repose, BD, TD, Carr's index, and HR.[10] For the determination of angle of repose (Θ), 5 g of the new crystals was accurately weighed and allowed to flow freely through a funnel previously fixed to a stand at a specific height (*h*). Angle of repose was determined using radius of the heap (*r*), and height of the powder using Equation (4). BD was determined by transferring 5 g of the new CUR crystal in a measuring cylinder and gently tapping it two times. The volume obtained was noted as "Vb." Similarly, TD was determined by transferring 5 g of powder into a measuring cylinder and tapping it 500 times. The volume was noted as "Vt." The weight of powder was measured and noted as "M." BD (ρb) and TD (ρt) were calculated by formulae given in Equations (5) and (6), respectively. Compressibility index (Carr's index) and HR of the prepared dry powder blends were calculated using the formulae given in Equations (7) and (8), respectively.

$$\theta = \tan^{-1}\left(h/r\right) \quad (4)$$

$$\rho b = M/V_b \quad (5)$$

$$\rho t = M/V_t \quad (6)$$

$$\text{Carr's index } (\%) = \left[TD - \left(BD/TD\right)\right] \times 100 \quad (7)$$

$$\text{Hausner's ratio} = TD/BD \quad (8)$$

Fourier-transform infrared spectroscopy. FT-IR spectra of unprocessed CUR, optimized batch of CUR crystal, pyrocatechol, and PEG 1500 were recorded on FT-IR (Shimadzu 8400S). Each sample (3 mg) was mixed with 4 mg of dry potassium bromide and compressed into disk under pressure of 10.000–15.000 psi. All the IR spectra were recorded at scanning range from 500 to 4,500 cm^{-1} and resolution of 16 cm^{-1}.[11,12]

Fourier transform proton nuclear magnetic resonance. The FT-^{1}HNMR spectrometer (model Advance-II Bruker) was used in the study. About 5–10 mg of unprocessed CUR crystal, optimized batch of CUR crystal, pyrocatechol, and PEG 1500 were individually placed in a glass tube and spun so as to subject the test material to uniform magnetic field strength of 9.4 T and ^{1}H frequency about 400 MHz along with automatic sample changer. The analyzed data were recorded through the computer attached to the nuclear magnetic resonance (NMR) instrument.

PXRD analysis. The PXRD patterns of unprocessed CUR crystal, optimized batch of CUR crystal, pyrocatechol, and PEG 1500 were recorded using X-ray diffractometer (X'PERT-PRO XRD is equipped with x'Celerator solid-state detector) along with the source of radiation "Cu line."[13] Standard runs were carried out using a generator setting of 45 kV voltage, 40 mA current, and scanning step time of 29.8450 s.

Diffraction scanning calorimetry. The thermal characteristics of unprocessed CUR crystal, optimized batch of CUR crystal, pyrocatechol, and PEG 1500 were evaluated using DSC (DSC Q200 Universal with V 24.4 software, Bangalore, India). Before DSC tracings, the instrument was calibrated for heat flow at temperature range of 25°C –300°C with nitrogen purging at about 50 mL/min. About 1–3 mg of samples were sealed in an aluminum crimped cell and tapped to make a uniform bed. An empty aluminum pan was used as reference standard. The samples were heated at a rate of 10°C/min.[12,14]

Scanning electron microscopy. The surface morphology of unprocessed CUR crystal, optimized batch of CUR crystal, pyrocatechol, and PEG 1500 was observed through digital SEM JSM-6100 (JEOL). Preparation of specimens was carried out as per the procedure reported by Patel *et al.*[12] and Renuka *et al.*[14] Samples were fixed onto a metallic stub with double-sided conductive tape (diameter) 29 mm, having an acceleration voltage of 10.0 kV with a secondary detector.

Preparation of Tablets

The unprocessed CUR crystals and optimized batch of CUR crystals were compressed into minitablets by direct compression. The drug and other suitable excipients, including diluent, disintegrant, and lubricant, were blended properly and finally compressed using dies and punches of 5 mm. Each ingredient was weighed accurately and mixed homogeneously using "V" cone blender. The blend was compressed using a tablet compression machine (Trover Pharmamach). Two different batches (B1 and B2) were prepared by varying the main drug ingredients. The unit formula composition for 50 mg tablet is shown in *Table 3*.

Postcompression Studies Related to Tablets

All the prepared formulations were evaluated for quality control parameters. The average thickness and diameter of the prepared tablets ($N = 10$) of two batches were measured using

Table 3. Unit Formula of Prepared Tablets

S. No.	Ingredients	B1	Ingredients	B2
1	CUR crystal	5	CUR (unprocessed)	5
2	Microcrystalline cellulose	17	Microcrystalline cellulose	17
3	Sodium starch glycolate	12	Sodium starch glycolate	12
4	Lactose	13	Lactose	13
5	Magnesium stearate	1.5	Magnesium stearate	1.5
6	Talc	1.5	Talc	1.5

All weights in the above table are in milligrams.

the Vernier caliper (Aerospace, Delhi, India). For weight variation, tablets ($N = 20$) from each batch were individually weighed and mean weight was calculated along with the percentage variation for each batch.[15] Tablet hardness was tested using a tablet hardness tester (Monsanto; H.L. Scientific Industries) for the determination of the average breaking strength of tablets. For each batch, tablets ($N = 10$) were tested and the mean of the response of hardness was recorded. To carry out the assay, tablets containing CUR crystals of Form-I and DCC equivalent to 5 mg were accurately weighed and dispersed in 10 mL of ethanol and dissolved properly. The solution was filtered through Whatman filter paper and the drug content therein was estimated by measuring absorbance at 420 nm. The procedure for other quality control tests for tablets is discussed in the following section.

Content Uniformity

The study was carried out as per Indian Pharmacopeia (IP) guidelines.[16] Tablets ($N = 10$) were taken and subjected to procedure individually. Each tablet was crushed in a mortar pestle and an accurately weighed amount of powder equivalent to the amount of drug (5 mg) in the formulation was dissolved in 250 mL of ethanol. The suspension was subjected to sonication until the drug got completely dissolved. The solution was filtered through Whatman filter paper, suitable dilutions were prepared, and the drug content was estimated by measuring absorbance at 420 nm. The tablets comply with the test if not more than one of the individual values thus obtained is outside the limits of 85%–115% of the average value and none is outside the limits of 75%–125%. If two or three individual values are outside the limits of 85%–115% of the average value, then the test will be repeated using another 20 tablets. The tablets comply with the test if in the total sample of 30 tablets, not more than three individual values should be outside the limits of 85%–115% and none should be outside the limits of 75%–125% of the average value.[16]

Friability testing. The study was carried out as per Zade *et al.*[17] Preweighed tablets ($N = 10$) from each batch were placed in the drum of a friabilator (Friability Testing Apparatus FT1020; LABINDIA, Mumbai, India) and rotated at 25 rpm for a period of 4 min. The final weight was measured and the percentage loss in weight was calculated as a measure of friability. The experiment was carried out in triplicate and mean response was recorded. The percentage friability was calculated as per the formula given in Equation (9).

$$\%\ \text{Friability} = \frac{\text{Initial weight} - \text{Final weight}}{\text{Initial weight}} \times 100 \qquad (9)$$

Disintegration testing. The study was carried out according to the method reported by Garg *et al.*,[15] using a disintegration apparatus (DT 10000; LABINDIA). The glass tubes were 3″ long, opened at the top, and 10 mesh screens at the bottom end. To test disintegration time, one tablet was placed in each tube and the basket rack was positioned in a 1 L beaker of water at 37°C ± 2°C such that the tablet remains 2.5 cm below the surface of liquid on the upward movement and not closer than 2.5 cm from the bottom of the beaker in the downward movement. The basket assembly was moved through a distance of 5–6 cm at a frequency of 28–32 cycles per minute. Floating of the tablets was prevented by placing a perforated plastic disc in each tube.

In vitro *dissolution studies.* The USP II (Paddle type) dissolution rate test apparatus LABINDIA D58000 was used for the study. Unprocessed CUR powder, optimized batch of CUR crystal powder, and their tablets were added to the vessels containing dissolution medium. The dissolution medium (900 mL distilled water) was stirred at 50 ± 4 rpm and temperature of the medium was maintained at 37°C ± 0.5°C, respectively. The study was carried out for 120 min. Samples equivalent to 5 mL were withdrawn at 15-min intervals from the dissolution medium, filtered, and their absorbance was recorded at 420 nm. The withdrawn medium was replaced by a fresh medium to maintain the sink condition. The studies were performed in hexaplicate and mean data (±standard deviation [SD]) were recorded.[18,19]

In Vivo Studies

High performance liquid chromatography method for pharmacokinetic studies. The developed and validated method reported by Kumar *et al.* was used in the present study for estimation of CUR in plasma samples.[20] The high performance liquid chromatography (HPLC) system (LC-20AD; Shimadzu) with photodiode array detector (SPDM20A; Shimadzu) with a 20 µL loop (Rheodyne) was used. LC solution software was used to

generate and analyze the data. CUR was estimated at 420 nm using acetonitrile (60% v/v) and 5% acetate buffer pH 2.35 (40% v/v) as the mobile phase at a flow rate of 1 mL/min. Before the start of the pharmacokinetic study, a bioanalytical method was developed for estimation of CUR in rat plasma. First, a blank plasma sample was injected to HPLC and then a 250 ng/mL drug solution (CUR) prepared in rat plasma was injected to check the possible effect of the matrix. This was followed by preparation of working standard (WS) solutions from the standard stock solution. The standard stock solution of CUR (1,000 μg/mL) was prepared by dissolving 50 mg of CUR in 50 mL of mobile phase. From the stock solution, an aliquot (10 mL) was withdrawn and then transferred to 100 mL of volumetric flask. The volume of the flask was adjusted to 100 mL with mobile phase. This was considered solution S1 (10 μg/mL). From the solution S1, 10 mL aliquot was withdrawn and transferred to another 100 mL volumetric flask and volume was adjusted to 100 mL using mobile phase. This was considered solution S2 (1 μg/mL). From the solution S2, 0.5, 1, 1.5, 2, and 2.5 mL of aliquots were withdrawn and transferred to 10 mL of the standard volumetric flask. To all these WS solutions, 0.5 mL plasma was spiked. The mixture was vortexed for about 10 min, acetone was added, and again vortexed for about 15 min. The mixture was then centrifuged at 1,000 rpm for 45 min. The supernatant was collected and evaporated. Reconstitution was done using mobile phase (10 mL) to achieve concentrations of 50, 100, 150, 200, and 250 ng/mL, respectively. The developed method was validated as per ICH Q2 (R1) guidelines for accuracy, precision, specificity, system suitability, and stability studies of the drug in plasma.[21] The method was found linear in the range of 50–250 ng/mL with coefficient of regression 0.9995, accurate with percentage recovery of 98.96, and precise with percentage relative SD <2%.

Pharmacokinetic studies. Albino Wistar male rats (7–8 weeks old) weighing 250–300 g were purchased from the National Institute of Pharmaceutical Education and Research (NIPER, Mohali, India) for the present study. Rats were housed in polypropylene cages lined with husk in standard environmental conditions (temperature 25°C ± 2°C, relative humidity [RH] 55% ± 10%, and 12:12 light:dark cycle). The animals were fed with standard pellet diet and water *ad libitum*. The experimental protocol was subjected to scrutiny, and ethical clearance was obtained from the Institutional Animal Ethics Committee of School of Pharmaceutical Sciences, Lovely Professional University (LPU/LSPS/IAEC/CPCSEA/MEETING No. 2/2017 Protocol No. 11) before beginning of the experiment.

For pharmacokinetic studies, twelve rats were divided into two groups, each containing six rats. The rats were treated as per a single crossover design in such a way that rats of both the groups were administered with both the treatments after a fixed washout period of 7 days. Unprocessed curcumin crystals (5 mg) and optimized curcumin crystals (5 mg) were administered orally to the rats based on the study design. Each study was carried out for 24 h. Each rat was anesthetized in an ether-saturated chamber and secured to a surgical board in a supine position with a thread. A polyethylene tube will be inserted into the right femoral artery of the rat. Then, 0.15 mL of blood was collected in EDTA vials from the right femoral artery at predetermined time intervals of 0, 1, 2, 3, 4, 5, 8, 12, 18, and 24 h and centrifuged at 1,000 rpm for 45 min using REMI CM-PLUS centrifuge (Remi Elekrdtechnik LTD), respectively, and plasma was separated out. Acetone (2 mL) was added to all the plasma samples (0.05 mL) and these were vortexed for 15 min to precipitate plasma matrix. The solution was centrifuged at 1,000 rpm for 45 min. The clear supernatant was collected in glass vials and evaporated at 60°C on a water bath. The dried samples were reconstituted in the mobile phase and injected to HPLC for analysis at 420 nm. Calculation of pharmacokinetic parameters such as area under the curve (AUC_{0-t} and $AUC_{0-\infty}$) was carried out using PK solver 2.0 software. The relative oral bioavailability was calculated by the formula given in Equation (10).

$$\text{Relative bioavailability (Fr)} = (AUC)_{test} \times D_{std} \div (AUC)_{std} \times D_{test} \quad (10)$$

where AUC is area under the curve and D is dose administered.

Stability Studies

The stability studies were carried out for optimized CUR crystal and its tablets at 40°C ± 2°C/75% RH ±5% RH, in stability chamber (Remi Electro Technique, Mumbai, India) for 6 months. The aged samples were analyzed and compared with results of freshly prepared crystals and their tablets for their size, assay, hardness, and friability at the end of 6 months. Freshly prepared crystals were considered time zero sample and used as a standard to evaluate various parameters of stability studies.

The dissolution studies of fresh and aged optimized CUR crystals were carried out in 900 mL of distilled water. The procedure to carry out dissolution has been discussed in the "Dissolution Studies" section. Each study was carried out six times and mean values (±SD) were recorded.

Statistical Analysis

All the experimental data are expressed as mean ± SD. The obtained results were compared by analysis of variance (ANOVA) or Tukey's multiple comparison test using GraphPad

Prism version 7.0 (GraphPad Software, Inc.). A value of $p < 0.05$ indicated significant difference in the obtained results. The dissolution profiles were compared using model independent analysis (f_2 comparison) as discussed by Shah *et al.*[22]

RESULTS AND DISCUSSION

A series of additives were explored for getting crystals of CUR with enhanced solubility profile (B1 to B12) as shown in *Table 1*. The results revealed a higher solubility of crystals that were obtained using pyrocatechol (15.55%) followed by PEG 1500 (11.45%). Solubility of crystals obtained using different additives was observed in the following increasing order:

Stearic acid < malonic acid < gallic acid < benzoic acid < oxalic acid < maleic acid < L-tartaric acid < SA < salicylic acid< CUR:SA: βCD < PEG 1500 < pyrocatechol.

It is important to note that the % yield of these crystals was found to be in the range of 70%–90%. Since the solubility was found maximum in case of crystals obtained using PEG 1500 and pyrocatechol, these were further explored for crystal growth by controlling different variables using BBD.

DESIGN OF EXPERIMENTS

According to BBD, 29 experiments were carried out to analyze the effect of pyrocatechol to PEG ratio, the speed of stirring, time of stirring, and addition rate on the responses, namely solubility (Y_1), Q_{120} (Y_2), percentage yield (Y_3), and particle size (Y_4). The responses of all the 29 experiments are shown in *Table 2*.

Among these experiments, maximum solubility of 56.98% and minimum solubility of 19.39% were observed for run 6 and run 4, respectively. Run 14 had the maximum Q_{120} % value of 100%, while run 4 had the minimum Q_{120} % value of 22.71%. Runs 5, 6, 11, 14, and 23 gave the maximum yield of 100%, while runs 1 and 29 gave the minimum yield of 20%. Run 28 produced maximum particle size of 8.61 μm and run 11 produced minimum particle size of 1.22 μm for CUR crystals. The ratio of maximum to minimum for Y_1, Y_2, Y_3, and Y_4 was 2.94, 4.24, 5, and 7.06, respectively. As these values were <10, hence the power of transformation was not required. Statistical analysis of the model was carried out by the design of experiments (DoE) tools such as the sequential model sum of squares and model summary statistics. The details of these tools are given in *Table 4*.

The lower value of SD, lower predicted residual error sum of square, high R-square, Prob > *F* value, and $p < 0.05$ indicated toward the selection of a linear model for responses Y_1 to Y_3 and quadratic model for Y_4. All the obtained results were analyzed through ANOVA. The results are shown in *Table 5*. The *F* value for responses Y_1, Y_2, Y_3, and Y_4 was found to be 3.97, 3.88, 3.89, and 2.91, respectively. This implied that the model was significant. Furthermore, the values of adequate precision for Y_1, Y_2, Y_3, and Y_4 were found to be 6.0131, 6.0416, 6.2877, and 8.159, respectively. This indicated that the applied model is adequate. The R-squared value was found to be above 0.400 for all the responses. Overall, all the obtained results of ANOVA revealed that the responses responded significantly to the independent variables. The lack of fit test *p*-value indicated that the responses of Y1, Y2, Y3, and Y4 were significant. The obtained polynomial equations for responses Y1, Y2, and Y3 are given in Equations (11)–(14), respectively.

$$\mathrm{Y1\ (Solubility)} = 38.14 + 11.89 * \mathrm{A} + 2.70 * \mathrm{B} + 1.33 * \mathrm{C} - 2.82 * \mathrm{D} \quad (11)$$

$$Y2\ (\mathrm{Q_{120}}) = 62.35 + 20.06 * \mathrm{A} + 4.85 * \mathrm{B} + 3.14 * \mathrm{C} - 5.62 * \mathrm{D} \quad (12)$$

$$\mathrm{Y3\ (Yield)} = 62.24 + 23.00 * \mathrm{A} + 7.08 * \mathrm{B} + 3.67 * \mathrm{C} - 1.25 * \mathrm{D} \quad (13)$$

$$\begin{aligned} Y4\ (\mathit{Particle\ size}) = {} & +3.56 - 0.12 * A - 1.13 * B - 0.013 * C \\ & + 0.16 * D - 0.89 * A * B + 0.16 * A * C \\ & + 1.19 * A * D - 1.27 * B * C - 0.29 * B * D \\ & + 0.16 * C * D - 0.44 * A2 + 0.53 * B2 \\ & + 0.28 * C2 - 0.69 * D2 \end{aligned} \quad (14)$$

Positive signs in the equations revealed the synergistic effect of factors on the responses. On the contrary, negative signs indicated the antagonistic effect of factors on the responses. In case of solubility (Y_1), Q_{120} (Y_2), and yield (Y_3), an increase in values was observed with an increase in pyrocatechol to PEG ratio, the speed of stirring, and time of stirring, while a decrease in values was observed with an increase in addition rate. Reverse was found in case of particle size (Y_4).

The three-dimensional graphs of response versus variables are presented in *Figures 1–3*. *Figure 1a* represents the effect of pyrocatechol to PEG 1500 ratio (A) and speed of stirring (B) on the solubility of CUR crystals. Drug's solubility was found to increase with increase in the ratio of factor A and stirring speed. Similar observations were found with an increase in pyrocatechol to PEG 1500 ratio (A) and stirring time (C) (*Fig. 1b*). As represented in *Figure 1c*, it was observed that the solubility of crystals decreased with an increase in solvent addition rate. This indicated that the amount of pyrocatechol has played a very important role in enhancing the solubility of optimized CUR crystals. In addition to that, the increase in stirring rate and stirring time could have provided better exposure of drug between solvent and antisolvent with enhanced agitation. This, in turn, would have further caused enhanced precipitation of small particles of CUR crystal.

Table 4. Statistical Analysis of the Model Using Design of Experiments Tools

Sequential model sum of squares

Source	Sum of squares				Df				Mean square				*F* value				*p*-Value (Prob > *F*)			
	Y_1	Y_2	Y_3	Y_4	Y_1	Y_2	Y_3	Y_4	Y_1	Y_2	Y_3	Y_4	Y_1	Y_2	Y_3	Y_4	Y_1	Y_2	Y_3	Y_4
Linear	1900.3	5609.5	7130.2	15.8	4	4	4	4	475.1	1402.4	1782.5	332.9	3.9	3.9	3.9	2.5	0.02	0.02	0.02	0.07
2FI	637.1	884.4	3801.5	15.8	6	6	6	6	106.2	147.4	633.6	1.7	2.6	0.33	1.7	2.2	0.55	0.91	0.20	0.09
Quadratic	544.1	2640.2	1766.9	8.1	4	4	4	4	136.0	660.0	441.5	1.0	2.0	1.8	1.2	2.1	0.39	0.21	0.36	0.14
Cubic	1202.3	3451.8	2897.8	9.8	8	8	8	8	150.3	431.5	362.2	0.7	1.22	3.4	1.1	1.88	0.03	0.25	0.58	0.23
Residual	9.8	254.3	690.1	3.88	2	2	2	6	4.9	127.1	345.0	0.3	–	–	–	–	–	–	–	–
Total	40663.1	1.100E+05	1.195E+05	53.4	24	24	24	28	16,26.5	4401.5	4778.2		–	–	–	–	–	–	–	–
Lack of fit tests																				
Linear	2200.5	7074.1	9190.8	36.7	20	20	20	20	110	353.7	459.5	1.83	0.46	0.47	0.49	8.40	0.8909	0.8864	0.8670	0.03
2FI	1563.3	6189.7	5389.3	20.9	14	14	14	14	111.7	442.1	384.9	1.49	0.4671	0.5846	0.4184	6.83	0.8705	0.7965	0.8995	0.04
Quadratic	1212.1	3706.1	3587.9	12.8	10	10	10	10	121.2	370.61	358.8	1.28	0.5070	0.4901	0.3900	5.85	0.8251	0.8357	0.8965	0.05
Cubic	9.8	254.3	690.08	3.01	2	2	2	2	4.9	127.1	345.0	1.50	0.02	0.17	0.38	6.89	0.98	0.85	0.71	0.05
Pure Error	956.3	3024.9	3680.0	0.87	4	4	4	4	239	756.2	920.0	0.22	–	–	–	–	–	–	–	–

Model summary statistics

	SD				R-squared				Adjusted R-squared				Predicted R-squared				PRESS			
Linear	11.47	20.51	23.16	1.25	0.38	0.36	0.36	0.30	0.27	0.2499	0.2492	0.18	0.1293	0.0912	0.0837	−0.09	4403.01	14276.70	18327.79	58.35
2FI	11.83	22.63	22.45	1.10	0.50	0.41	0.55	0.60	0.22	0.0875	0.2946	0.37	−0.1654	−0.4992	−0.0869	−0.03	5893.29	23550.00	21739.31	70.05
Quadratic	12.45	21.93	22.78	0.99	0.57	0.57	0.64	0.74	0.14	0.1430	0.2732	0.50	−0.6761	−0.6598	−0.3208	−0.40	8475.94	26073.43	26416.40	74.84
Cubic	12.69	23.38	26.99	0.80	0.81	0.79	0.78	0.93	0.11	0.02	−0.02	0.70	0.42	−1.63	−4.25	−7.15	2907.72	41343.4	1.051E+05	434.5

2FI, two-factor interaction; PRESS, predicted residual error sum of square; SD, standard deviation.

Table 5. Analysis of Variance Results of the Model Using Design of Experiments Tools

ANOVA				
Terms	**Y_1**	**Y_2**	**Y_3**	**Y_4**
F-calculated	3.97	3.88	3.89	2.91
p-Value	0.0157	0.0172	0.0170	0.0273
Lack of fit *p*-values	0.8909	0.8864	0.8670	0.0518
R-squared	0.4426	0.4369	0.4378	0.7445
Adjusted R-squared	0.3311	0.3242	0.3254	0.4889
Predicted R-squared	0.1556	0.1161	0.1073	−0.4032
Adequate precision	6.0131	6.0416	6.2877	8.159
PRESS	3625.54	11349.75	14539.27	74.84
SD	10.94	19.01	21.40	0.99

ANOVA, analysis of variance.

However, when the solvent addition rate was higher, poor interaction of solvent to antisolvent would lead to the generation of larger crystals of CUR with poor solubility compared with that of the crystals produced at a lower solvent addition rate. An increase in percentage drug solubility was observed with increase in stirring speed and time (*Fig. 1d*). *Figure 1e* represents the effect of addition rate (D) and time of stirring (C) and *Figure 1f* represents the effect of stirring speed (B) and solvent addition rate (D) on percentage CUR solubility. The study confirmed that the increase in pyrocatechol to PEG ratio, the speed of stirring and time of stirring increased Q_{120}, while an increase in addition rate decreased Q_{120}.

Similar results were observed for Q_{120} (Y_2) and crystal's yield (Y_3) in which it was observed that with the increase in pyrocatechol to PEG 1500 ratio (A), stirring speed (B), and stirring time (C), both Y_2 and Y_3 values were found to increase, whereas with increase in the solvent addition rate (D) their values got decreased. *Figure 2a and b* shows the effect of pyrocatechol to PEG 1500 ratio (A) and stirring speed (B) on Q_{120} (Y_2) and yield (Y_3), respectively. It was observed that with an increase in the values of factors A and B, the responses Y_2 and Y_3 gradually increased. Similar results are shown in *Figure 2c and d* for responses Y_2 and Y_3 with an increase in factors A and C. However, a gradual decrease in response Y_2 and Y_3 was observed with an increase in factor C (*Fig. 2e, f*).

In case of particle size (Y_4), a decrease in response was observed with increase in pyrocatechol to PEG 1500 ratio (A), stirring speed (B), stirring time (C), whereas the size was found to decrease with decrease in feed rate (*Fig. 3a*–f). It is a known fact that at higher speed, the shear rate is found more to break the particles to micron or submicron level. This effect was accelerated by an increase in the time of mixing and slow feed rate because these allowed better interaction between solvent and antisolvent that caused slower drug precipitation with a higher agitation rate.

Optimization of Variables by Graphical Method

Optimization of the formulation was carried out to find the levels of factors A-D, which resulted in Y_1 (solubility) in the range of 38%–56.98%; Y_2 (Q_{120}) in the range of 85%–100%; Y_3 (yield) in the range of 60%–100%, and Y_4 in the range of 1.22–8.61 μm, respectively. Graphical optimization method was used to predict Y_1 to Y_4 in the required range at A, B, C, and D values of 0.66, 1,500 (rpm), 75 (min), and 0.15 (mL/min), respectively, with desirability of 0.987. By using the suggested values of factors, three different batches of CUR crystals were prepared. The obtained values for solubility was 61.35% ± 3.12%, Q_{120} was 90.22% ± 1.22%, yield was 85.79% ± 4.32%, and size were 2.45 ± 0.56 μm, which were in close agreement to the predicted values (*i.e.*, $Y_1 = 52.97\%$; $Y_2 = 87.98\%$; $Y_3 = 86.42\%$; $Y_4 = 2.68$ μm).

Micromeritic Studies of the Optimized Crystal Form

The angle of repose values for unprocessed CUR crystal and optimized CUR crystals were 30.09° ± 0.5° and 26.1 ± 0.2°; BD: 0.66 ± 0.006 and 0.74 ± 0.006 g/cm^3; TD: 0.74 ± 0.02 and 0.87 ± 0.01 g/cm^3; Carr's index 21.71 ± 1.21 and 14.57 ± 0.66; and HR 1.24 ± 0.001 and 1.16 ± 0.02, respectively. It was observed that the optimized crystal had better compaction properties compared with the unprocessed crystal as the values of angle of repose, bulk, and TD were less and Carr's index and HR were high for it compared with the unprocessed one. However, the difference between these parameters for both the crystal forms was not found to be significant.

Fourier-Transform Infrared Spectroscopy

FT-IR provides useful information about the vibrational modes of a molecule resulting from changes in the physical state of the sample and differences in hydrogen bonding and molecular conformations.[23] Hydroxyl groups were found to be absorbed strongly in the 3,700–3,584 cm^{-1} region. Phenolic and olefinic C-O stretching vibrations occurred between 1,260, 1,000, and 1,430–1,410 cm^{-1}, respectively.[23] The IR vibrational frequencies of optimized curcumin crystals as well as those of unprocessed curcumin and the excipients are given in *Table 6*. The changes in the O-H overtone, keto —C(=O)—, enol HO—, and —O—CH stretching frequencies of the optimized crystals compared with the constituents suggested the formation of a new crystal form. However, the peaks related to

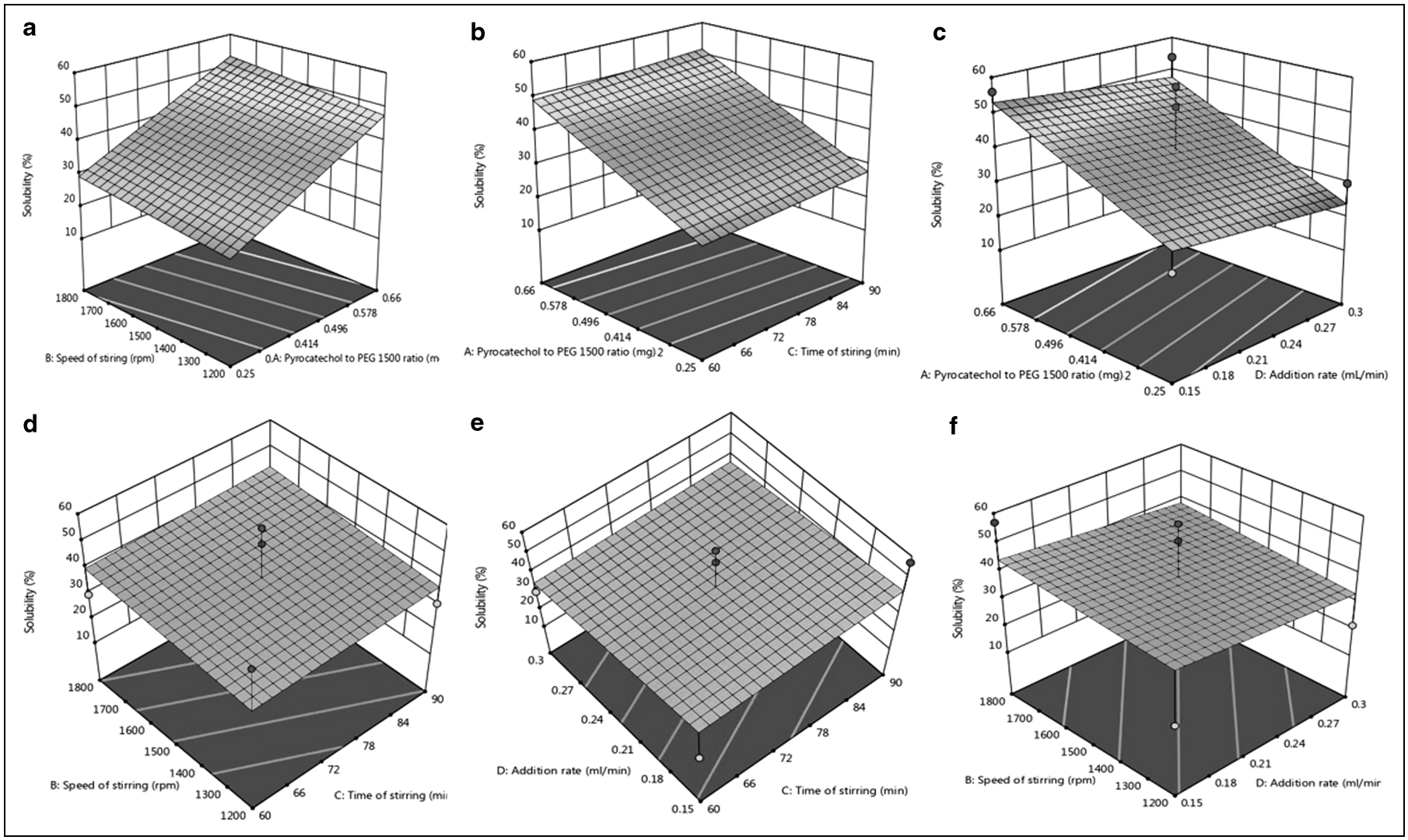

Fig. 1. Effect of variables on crystal's solubility (Y_1); **(a)** catechol to polyethylene glycol ratio (A) and speed of stirring (B); **(b)** catechol to polyethylene glycol ratio (A) and time of stirring (C); **(c)** catechol to polyethylene glycol ratio (A) and feed rate (D); **(d)** speed of stirring (B) and time of stirring (C); **(e)** time of stirring (C) and feed rate (D); **(f)** speed of stirring (B) and feed rate (D).

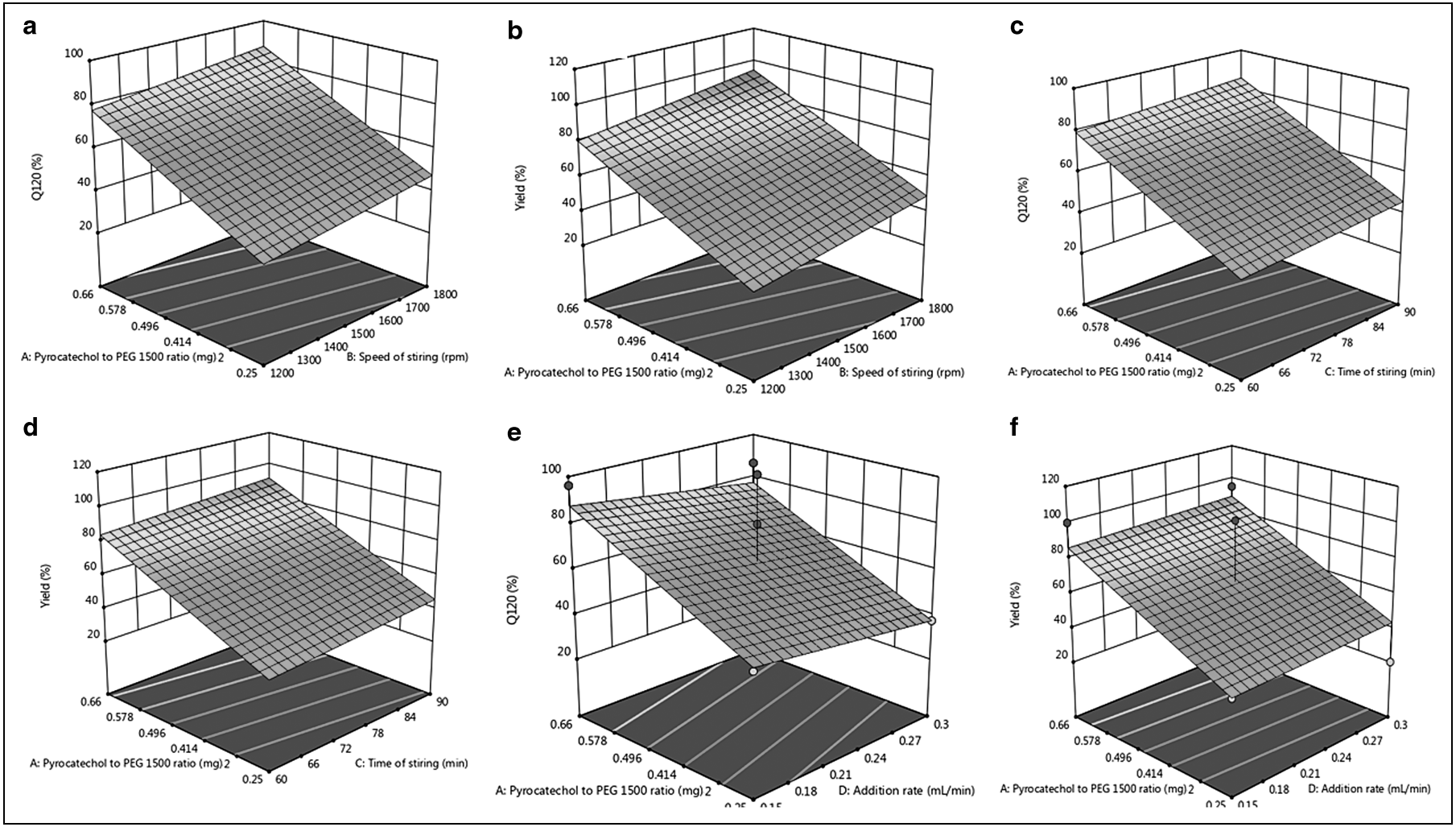

Fig. 2. Effect of variables on crystal's Q120 (Y_2) and yield (Y_3); **(a)** catechol to polyethylene glycol ratio (A) and speed of stirring (B) on Y_2; **(b)** catechol to polyethylene glycol ratio (A) and speed of stirring (B) on Y_3; **(c)** catechol to polyethylene glycol ratio (A) and time of stirring (C) on Y_2; **(d)** catechol to polyethylene glycol ratio (A) and time of stirring (C) on Y_3; **(e)** catechol to polyethylene glycol ratio (A) and feed rate (D) on Y_2; **(f)** catechol to polyethylene glycol ratio (A) and feed rate (D) on Y_3.

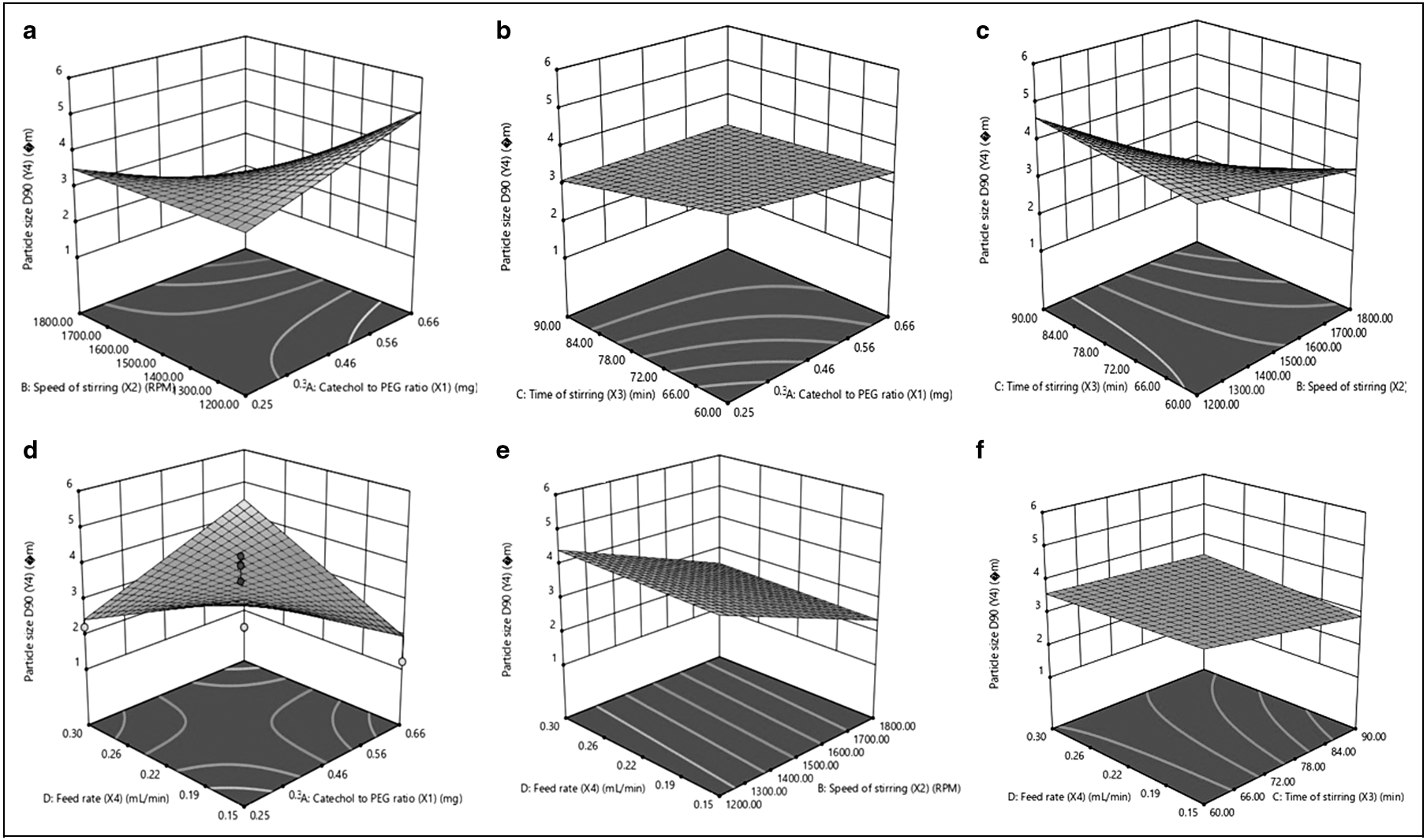

Fig. 3. Effect of variables on crystal's size on Y_4; **(a)** catechol to polyethylene glycol ratio (A) and speed of stirring (B); **(b)** catechol to polyethylene glycol ratio (A) and time of stirring (C); **(c)** speed of stirring (B) and time of stirring (C); **(d)** catechol to polyethylene glycol ratio (A) and feed rate (D); **(e)** speed of stirring (B) and feed rate (D); **(f)** time of stirring (C) and feed rate (D).

Table 6. Fourier Transform Infrared Stretching Vibration Mode Wavenumber ($v \cdot cm^{-1}$) for Unprocessed Curcumin Crystal and Optimized Curcumin Crystal

Samples	O-H	CH	Overton, O=C	Keto, O=C	Aromatic, C=C—H	Enol, HO—	—O—CH
Unprocessed curcumin	3509.6	2924.18	2359.98	1627.97	1601.93	1428.34	1280.78
Pyrocatechol	3452.70	3053.42	2733.22	1609.65	1368.54	–	–
PEG 1500	3426.66	2880.78	–	–	–	–	–
Developed curcumin crystal	3411.22	3044.74	2360.95	1627.01	1587.01	1460.16	1291.39

pyrocatechol and PEG 1500 were not found in the newly developed crystals. This fact suggested that these excipients played only a catalytic effect that helped to change the crystalline structure of CUR.

Fourier Transform Nuclear Magnetic Resonance

In *Figure 4a* and *b*, the characterized spectra obtained in ^{1}H NMR (400 MHz), dimethyl sulfoxide (DMSO), δ (ppm) at 3.82 (s, 3H, OCH_3), 3.84 (s, 3H, OCH_3), 5.88 (s, 1H, enol), 6.54 (d, J= 15.8Hz, 2H), 6.81 (d, J= 8.12 Hz, 2H), 7.03 (dd, J= 7.12Hz, 0.88Hz, 2H), 7.13 (s, 2H), 7.49 (d, J= 15.76 Hz, 2H), 9.36 (s, 2H, OH) for unprocessed CUR.

In *Figure 5a* and *b*, the characterized spectra obtained in ^{1}H NMR (400 MHz), DMSO, δ (ppm) at 6.61–6.66 (m, 2H), 6.77–6.81 (m, 2H) for obtained crystals of curcumin.

In *Figure 6a* and *b*, the characterized spectra obtained in ^{1}H NMR (400 MHz), DMSO, δ (ppm) at 3.34 (s, OH), 3.47–3.42 (m, CH_2) for pyrocatechol.

In *Figure 6c*, the characterized spectra obtained in ^{1}H NMR (400 MHz), DMSO, δ (ppm) at 3.84 (s, 6H, $2OCH_3$), 6.06 (s, 1H, enol), 9.66 (s, 2H, OH) for PEG 1500.

From the above NMR studies of unprocessed CUR, excipients along with the optimized curcumin crystals, it was concluded that two methoxy (OCH_3; 3.82 ppm) and (3.84 ppm) singlet spectra were observed in unprocessed CUR, whereas in case of newly developed crystal, one singlet of two methoxy group (3.84 ppm) was observed. The enol hydrogen observed in case of unprocessed CUR at 5.88 ppm has a singlet spectrum in which a developed CUR crystal was observed at 6.06 ppm. Also, the phenolic OH of unprocessed CUR was observed at 9.36 ppm, whereas in developed CUR crystals it was observed at 9.66 ppm.

PXRD Analysis

The PXRD patterns of unprocessed CUR, pyrocatechol, PEG 1500, and optimized curcumin crystal are shown in *Figure 7a*–d, respectively. All the samples revealed sharp peaks. The crystalline peaks of unprocessed CUR were observed at 7.85°, 8.86°, 12.14°, 14.48°, 17.24°, 18.07°, 21.09°, 23.30°, 23.73°, 24.47°, 25.48°, 26.04°, 26.89°, 27.30°, and 28.90° 2Θ, respectively, at their corresponding relative intensities of 13.26%, 88.35%, 21.94%, 34.83%, 100%, 37.96%, 22.98%, 35.97%, 29.74%, 34.54%, 40.57%, 23.06%, 16.88%, 28.98%, and 22.55%, respectively (*Fig. 7a*). The crystalline peaks of pyrocatechol were observed at 9.91°, 18.43°, 19.94°, and 25.71° 2Θ, respectively, with their relative intensities of 100%, 26.29%, 16.26%, and 62.02%, respectively (*Fig. 7b*). The single sharp crystalline peak at 19.27° 2Θ at 100% relative intensity was observed for PEG 1500 (*Fig. 7c*).

It is important to note that the crystalline peaks of newly formed crystals were different from that of unprocessed crystals, as revealed by the diffraction patterns. The crystalline peaks of developed crystals were observed at 13.91°, 17.70°, 25.18°, 26.25°, and 26.69° 2Θ with the corresponding relative intensity of 100%, 23.53%, 20.18%, 85.14%, and 41.24%, respectively (*Fig. 7d*). These results indicated the formation of new crystals of CUR. Moreover, the absence of crystalline peaks at diffraction angles of pyrocatechol and PEG 1500 revealed that they only helped as a catalyst. It is also important to note that developed crystals were less crystalline in comparison with unprocessed curcumin crystals, as observed by the appearance of a greater number of peaks in diffractogram of unprocessed form compared with that of newly developed crystals with higher counts, that is, up to 5,000 for unprocessed form and up to 2,500 for newly developed crystals. The decrease in crystallinity of optimized CUR crystals would have contributed to the enhancement of the aqueous solubility compared with that of unprocessed form.[24]

Diffraction Scanning Calorimetry

The DSC of unprocessed CUR crystals, pyrocatechol, PEG 1500, and optimized CUR crystals is shown in *Figure 8a–d*. The signal for sharp melting peak of unprocessed CUR crystals was observed at 178.80°C, whereas for optimized crystals, the melting endotherm appeared at a lower temperature (164.44°C). The energy required for melting of unprocessed CUR crystals was 139.4 J/g,

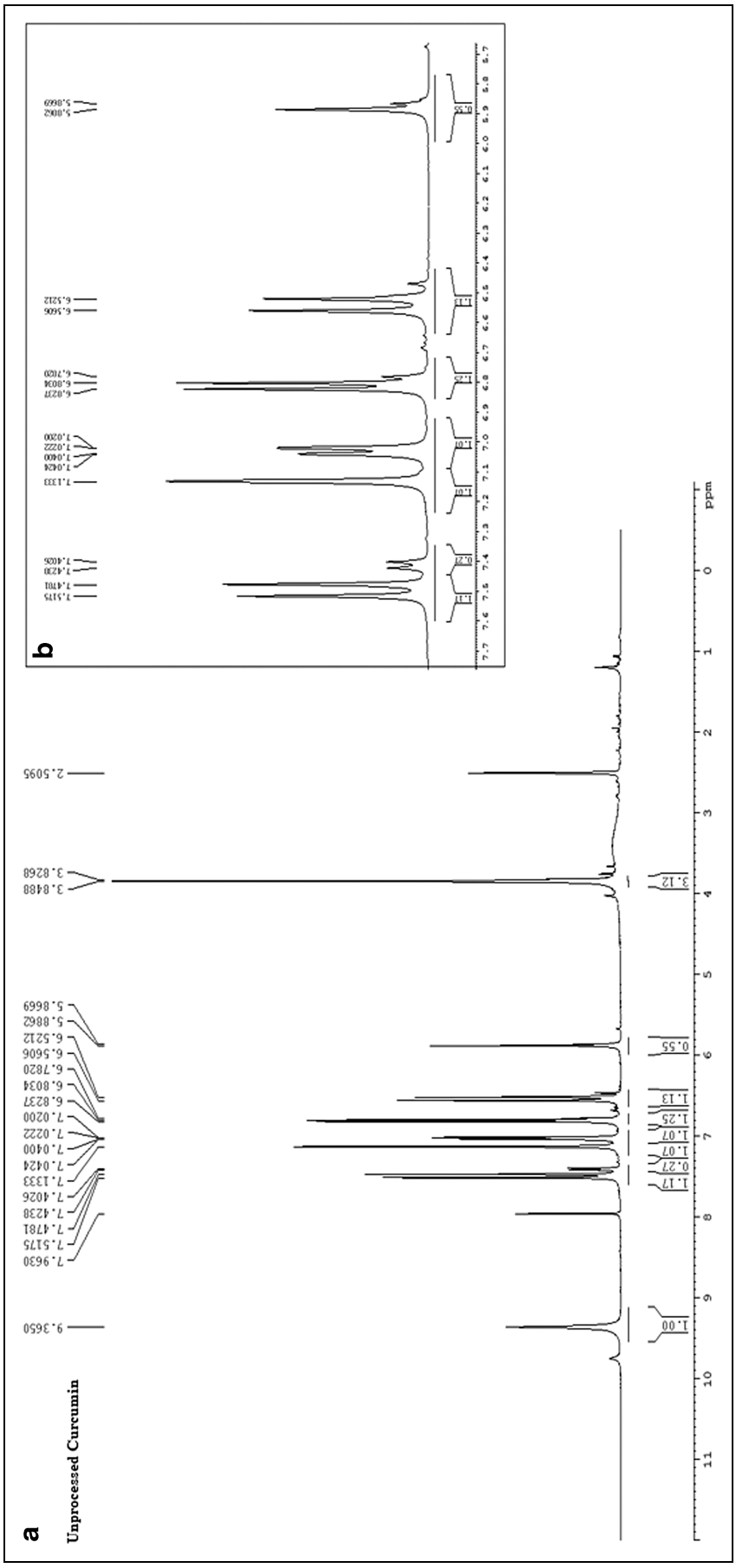

Fig. 4. Complete Fourier transform proton nuclear magnetic resonance spectrum **(a)** and splitted spectrum **(b)** of unprocessed curcumin.

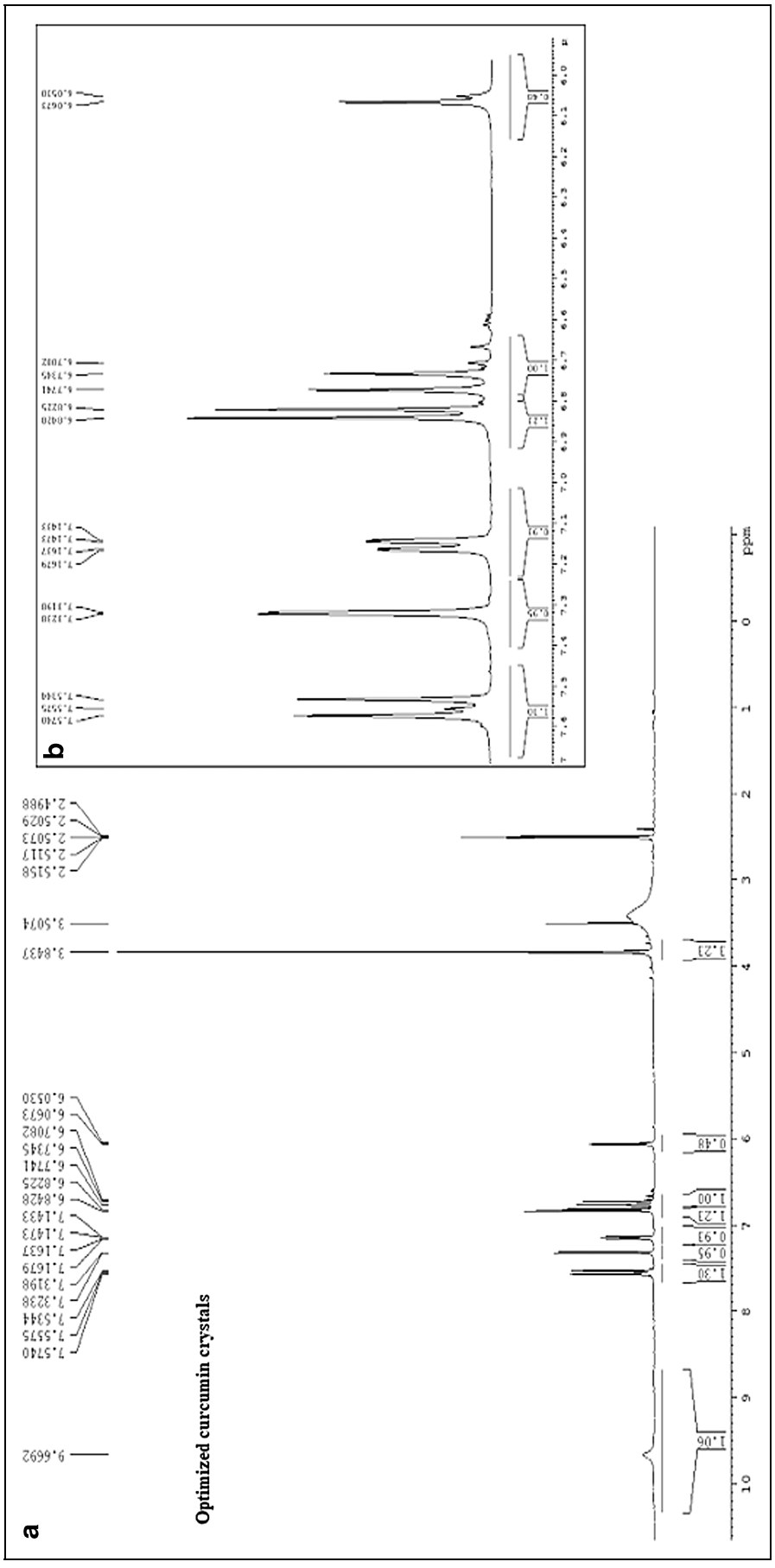

Fig. 5. Complete Fourier transform proton nuclear magnetic resonance spectrum **(a)** and splitted spectrum **(b)** optimized curcumin crystals.

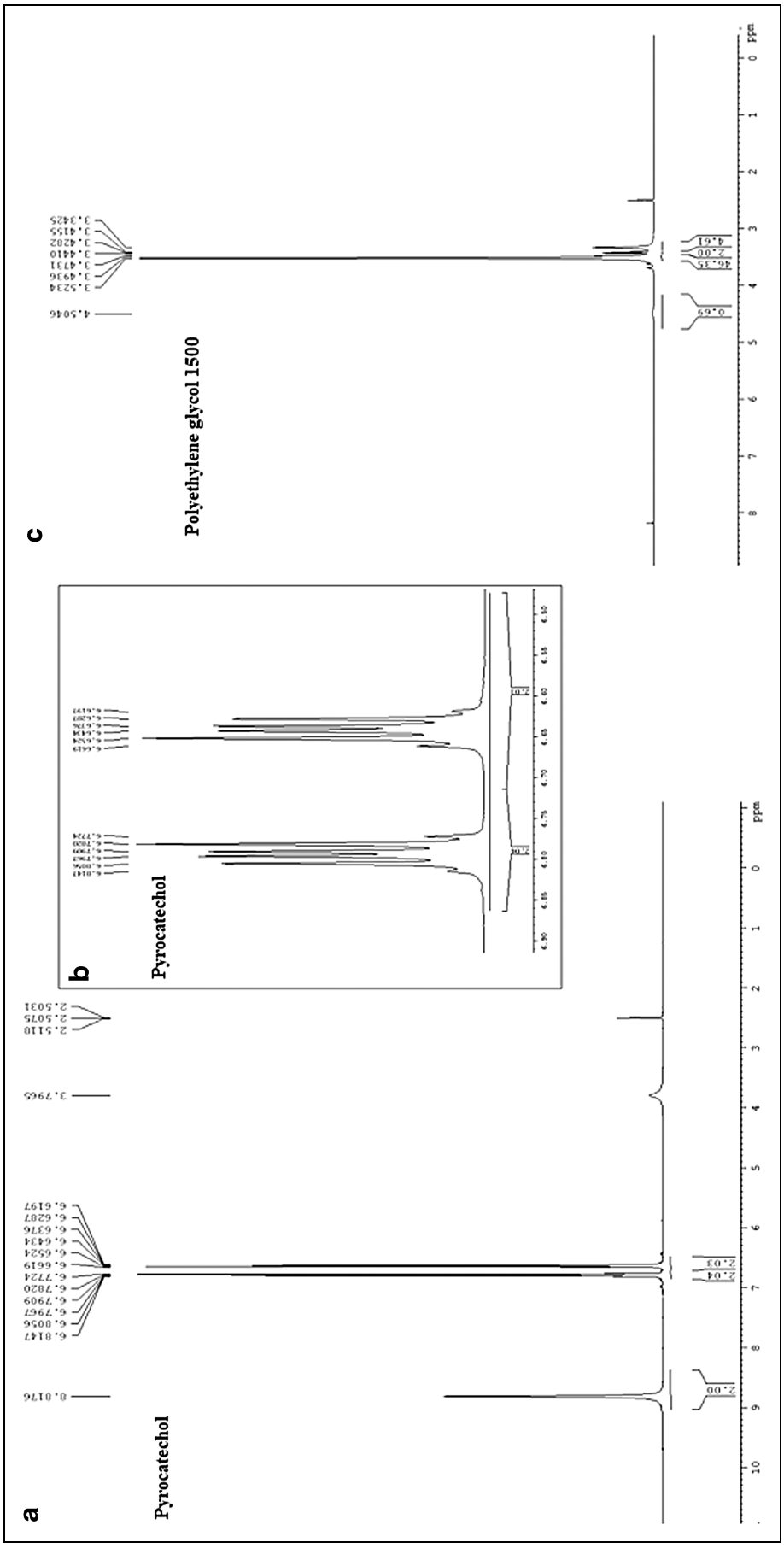

Fig. 6. Complete Fourier transform proton nuclear magnetic resonance spectrum of pyrocatechol **(a)** and splitted spectrum of pyrocatechol **(b)**; polyethylene glycol 1500 **(c)**.

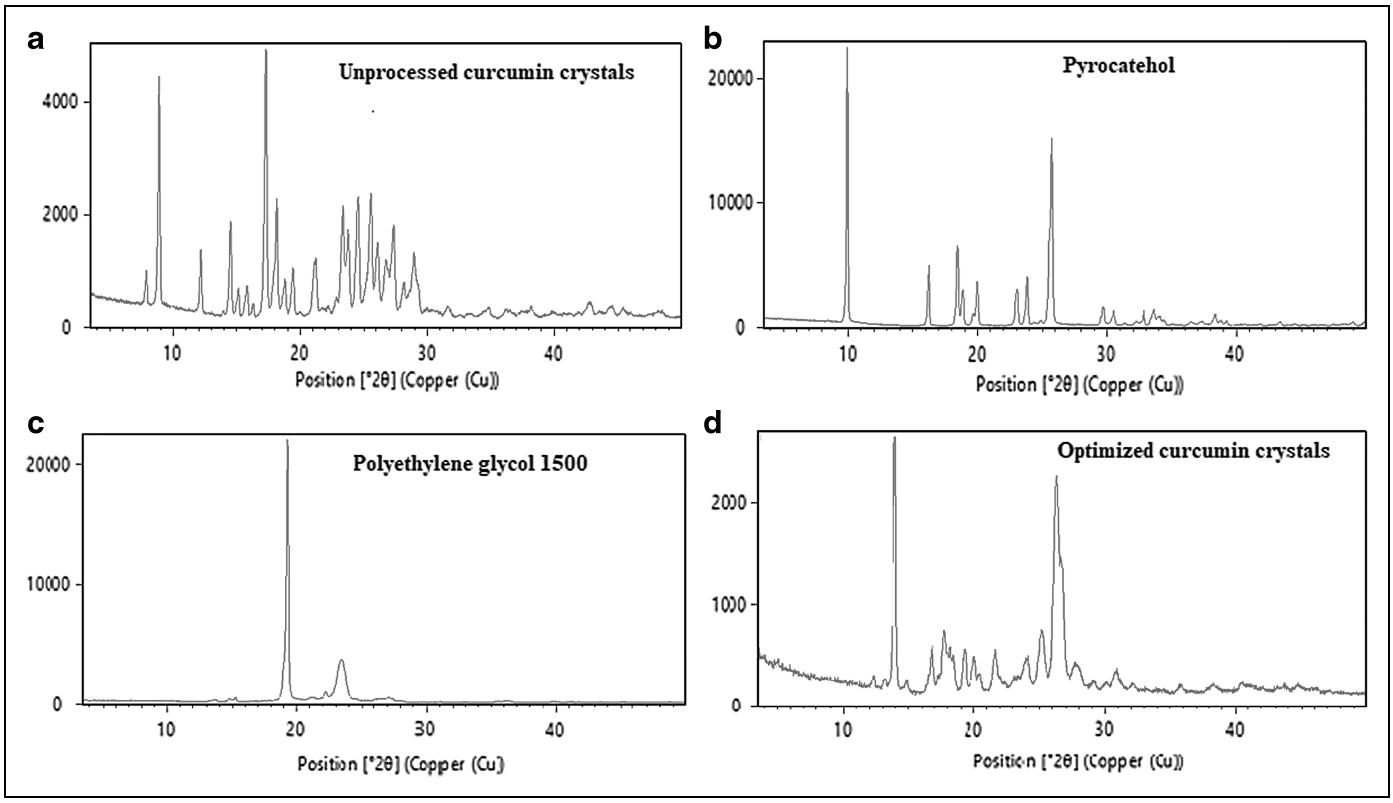

Fig. 7. Powder X-ray diffractions patterns of **(a)** unprocessed CUR crystals; **(b)** pyrocatechol; **(c)** polyethylene glycol 1500; **(d)** optimized curcumin crystals. CUR, curcumin.

whereas the energy required for melting of optimized CUR crystals was 28.26 J/g. The energy required for optimized CUR crystals was much lower compared with that for the unprocessed form, indicating less crystallinity of optimized crystals. Hence, the results of PXRD and DSC studies indicated different intramolecular packings of both the CUR forms. The excipients just acted as catalysts to generate the crystal with enhanced solubility. As reported in the literature,[25] the first endothermic peak in the DSC curve indicated polymorphic transformation of orthorhombic form (optimized CUR crystal) to monoclinic (unprocessed CUR crystal) and the second peak corresponded to the melting of unprocessed form.

It is important to note that the crystals obtained through LAP may contain the residual solvents in their crystal lattice. In the present study, ethanol was used as organic solvent. The absence of desolvation peak at the boiling point of ethanol (*i.e.*, 78°C–80°C) in the DSC thermogram of optimized CUR cocrystals (*Fig. 8d*) indicated that the obtained cocrystals were free from any residual solvents.

Scanning Electron Microscopy

Unprocessed CUR crystals appeared as flat, blade-like smooth-surfaced rectangular crystals having sharp irregular edges, indicating a monoclinic form (*Fig. 9a*). Pyrocatechol appeared as long thread-like networks having waxy appearance (*Fig. 9b*), whereas PEG 1500 appeared as unorganized waxy mass (*Fig. 9c*). The SEM of optimized CUR crystal showed long and pointed sharp acicular needles indicating orthorhombic form (*Fig. 9d*). This difference in crystal habit between unprocessed CUR crystals and optimized CUR crystals can be attributed to the difference in the environmental conditions for growth of both the crystals.[14] This led to the generation of crystals with different shapes but the same internal structure. It is important to note that absence of waxy appearance in SEM of both the forms indicated the absence of PEG 1500 and pyrocatechol. This indicated that both the additives provided only catalytic activity during the crystal growth of optimized CUR crystal in ethanol and confirmed the findings recorded through FT-IR, FT-NMR, PXRD, and DSC studies.

Postcompression Studies Related to Tablets

All the formulations were evaluated for quality control parameters that are shown in *Table 7*. After the evaluation of all the parameters, it was found that the assay of curcumin

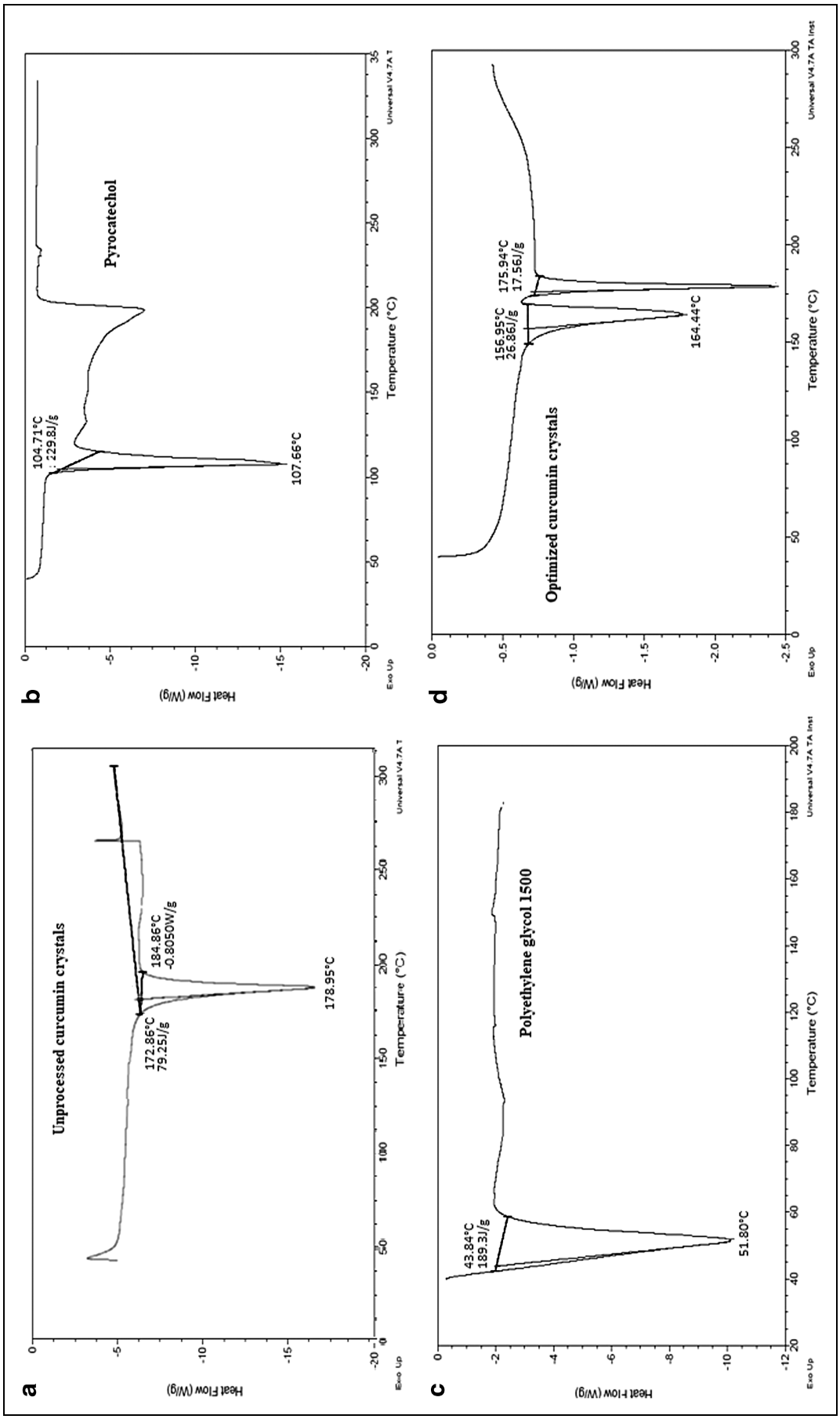

Fig. 8. Differential scanning thermograms of **(a)** unprocessed curcumin crystals; **(b)** pyrocatechol; **(c)** polyethylene glycol 1500; **(d)** optimized curcumin crystals.

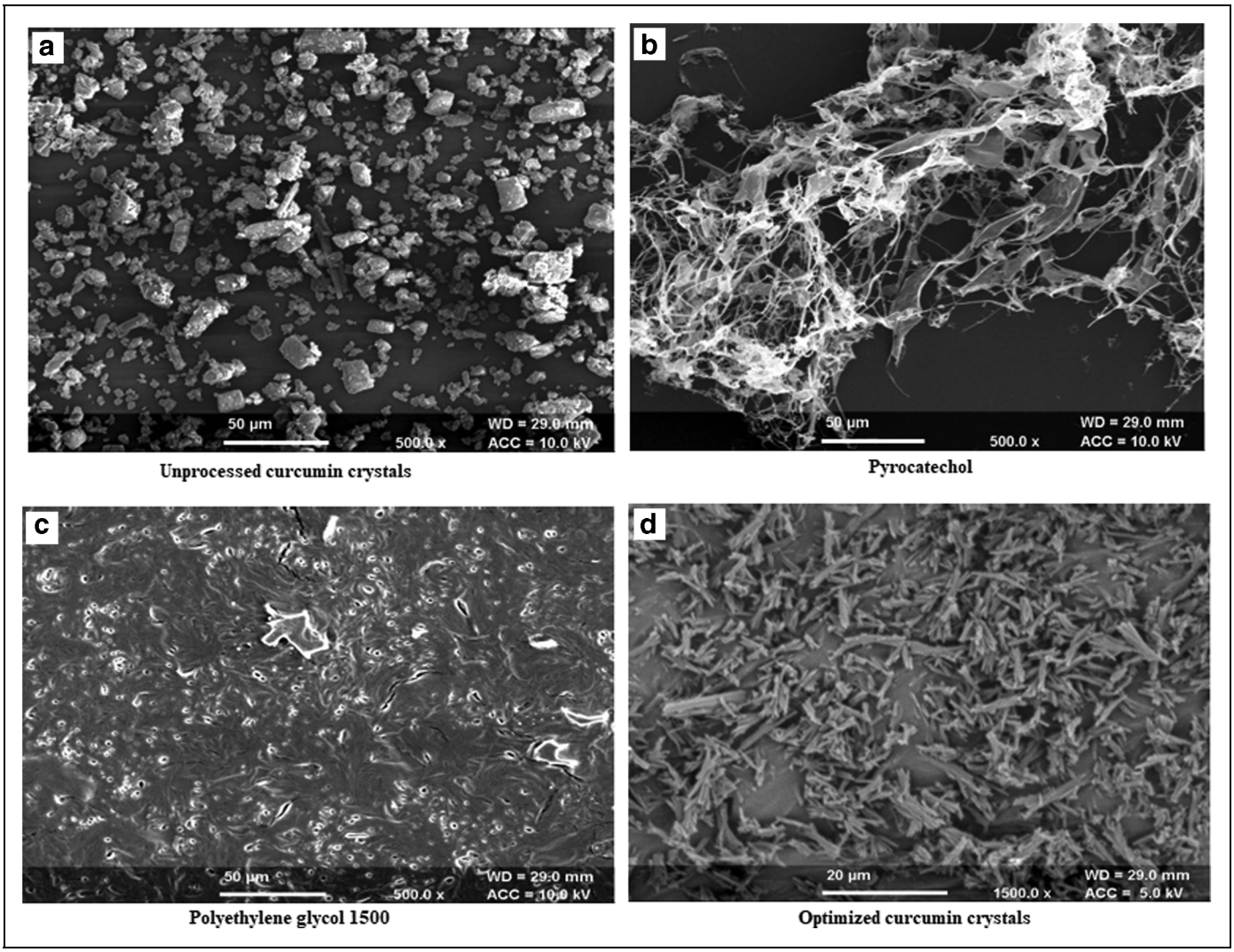

Fig. 9. Scanning electron microscopic images of **(a)** unprocessed curcumin crystals; **(b)** pyrocatechol; **(c)** polyethylene glycol 1500; **(d)** optimized curcumin crystals.

Table 7. Postcompression Quality Control Parameters Related to Tablets

Batches	Appearance	Thickness (mm)	Diameter (mm)	Content uniformity (%)	Weight variation (mg)	Friability (%)	Hardness (kg/cm^2)	Disintegration time (min)	Assay (%)
Unprocessed CUR tablet	Round shaped, pale-yellow color	1.99 ± 0.006	4.35 ± 0.006	91.25 ± 3.042	± 4.8	0.25 ± 0.52	3.4 ± 0.06	5.11 ± 0.005	92.22 ± 3.051
Optimized CUR crystal tablet	Round shaped, bright yellow-orange color	1.98 ± 0.008	4.34 ± 0.008	92.94 ± 4.012	± 5.0	0.80 ± 0.32	3.5 ± 0.06	5.14 ± 0.006	93.44 ± 3.347

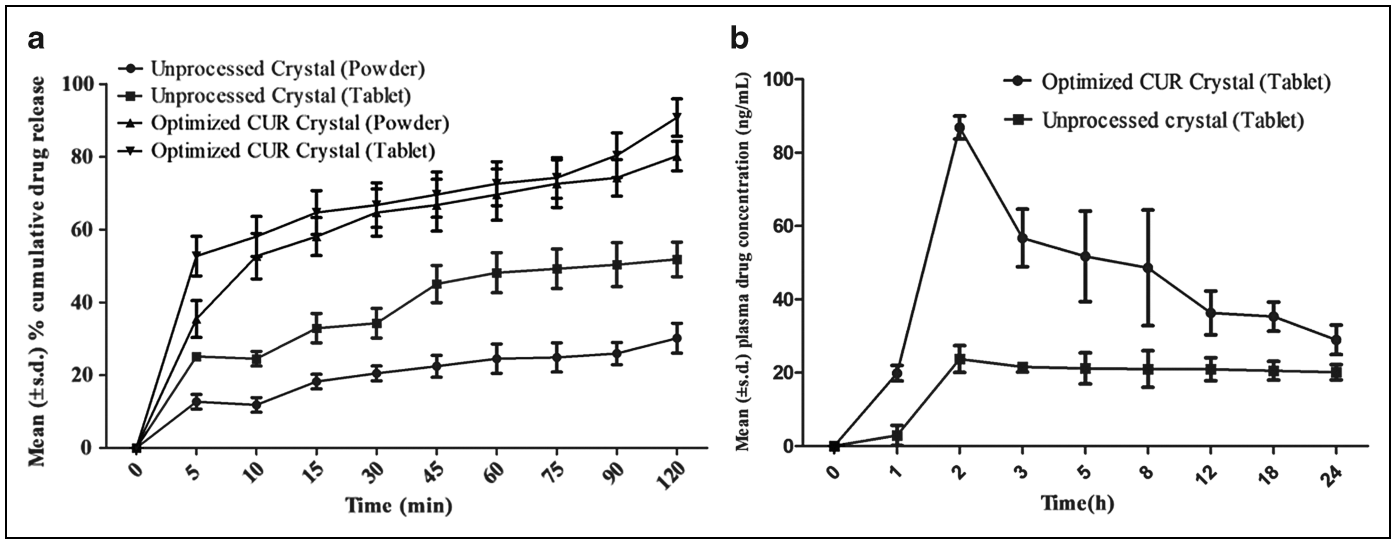

Fig. 10. **(a)** *In vitro* powder and tablet dissolution profile of unprocessed curcumin crystal and optimized curcumin crystals; **(b)** plasma drug concentration versus time profile of unprocessed curcumin crystals and optimized curcumin crystals (tablet).

present in the unprocessed CUR tablet was 92.22% ± 3.051% and in optimized CUR tablet, it was 93.44% ± 3.347%. The hardness was found to be 3.4 ± 0.06 kg/cm^2 and 3.5 ± 0.06 kg/cm^2 for unprocessed CUR tablet and optimized CUR tablet, respectively, friability (%) was found to be <1% for all the tablets and weight variation was within the pharmacopeial acceptance limits ±5.0%.[15] Also, the disintegration time for tablets of both crystals was nearly similar, that is, 5.11 ± 0.005 and 5.14 ± 0.006.

In Vitro Dissolution Studies

The dissolution studies were carried out for unprocessed CUR powder and its tablets, as well as for optimized CUR powder and its tablets, for 120 min. The study revealed poor dissolution profile of unprocessed CUR crystals compared with that of optimized CUR crystals through their powder as well as tablet formulations. The drug release for the unprocessed form from its powder and tablets was found to be 30.19% and 51.83%, respectively, in 120 min, whereas it was found to be 80.22% and 90.79% for optimized CUR form from powders and tablets, respectively, in 120 min. The results are shown in *Figure 10a*. Hence, about 2.66-fold increase in drug release was observed for optimized CUR powder as that of unprocessed CUR powder, whereas it was about 1.76-fold increase in drug release from optimized CUR tablets as that of unprocessed CUR tablets.

This reflected a significant increase ($p < 0.05$) between the dissolution profiles of optimized CUR powder and tablets compared with their unprocessed form (the p-value of unprocessed CUR powder vs. optimized CUR powder was 0.019 and unprocessed CUR tablet vs. optimized CUR tablet was 0.035). Unprocessed CUR crystals, being hydrophobic and more crystalline in nature did not allow the dissolution medium to completely wet the particles and thereby the particles remained floating on top of the surface of the dissolution medium and very less drug got released. When optimized CUR crystals were added in the medium, they did not rise up in the dissolution medium, moreover, they started dissolving in the medium very fast and almost got solubilized at the end of 120 min.

Pharmacokinetic Studies

The *in vivo* crossover pharmacokinetic studies were carried out on rat and results revealed that the drug release started immediately after its oral administration. At the end of 2 h, plasma concentration of unprocessed CUR tablets was 23.73 ng/mL, while it was 86.87 ng/mL for optimized CUR tablets. A 3.66-fold greater absorption was observed for optimized CUR tablets compared with unprocessed CUR tablets. The T_{max} for both the forms was 2 h. The AUC_{0-t} and $AUC_{0-\infty}$ were found to be 474.17 and 6536.06 ng/mL × h for

Table 8. Results of Stability Studies

Sample	Assay	Hardness	Friability
Fresh CUR tablets	93.44 ± 3.347	3.5 ± 0.06	0.80 ± 0.32
Aged CUR tablets	92.38 ± 0.32	3.1 ± 0.14	0.90 ± 0.01
p-Value (aged vs. fresh)	0.16	0.45	0.09

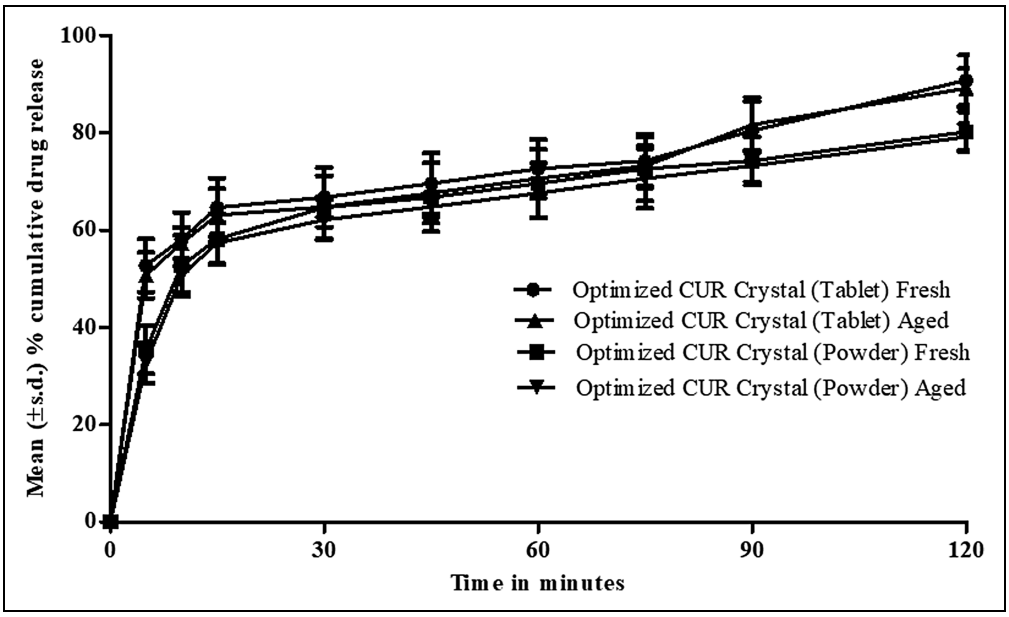

Fig. 11. Dissolution profile of fresh and aged optimized curcumin crystal's powder and its tablet.

unprocessed CUR crystals and 971.65 and 1889.86 ng/mL × h for optimized CUR crystals, respectively. The relative bioavailability for the unprocessed CUR crystals was 7.25%, whereas it was 51.40% for optimized CUR crystals. About a 7.08-fold increase in bioavailability was observed for optimized CUR crystals as that of unprocessed CUR crystals. The overlay of the plasma concentration versus time curve for both the forms is shown in *Figure 10b*.

Stability Studies

The accelerated stability studies revealed no significant change ($p > 0.05$) in the size, assay, hardness, and friability at the end of first, third, and sixth month of optimized crystal compared with fresh one (*Table 8*). The initial size was 2.45 ± 0.56 μm and after stability studies, it was found to be 3.05 ± 0.87 μm. This slight increase in the particle size did not affect the dissolution profile of the drug as the *p*-values between aged and fresh CUR crystals in powder form as well as in tablets were found to be 0.49, which was more than 0.05 (*Fig. 11*). Moreover, the f2 values were 61.75 and 64.97 for powder and tablet dissolution profiles indicating similar dissolution profiles. The absence of significant difference in size, assay, hardness, friability, and dissolution rate of obtained fresh and aged crystals confirmed the physical stability of developed crystals.

CONCLUSION

The study was undertaken to control generation of CUR crystals using the QbD approach with enhanced dissolution rate and oral bioavailability. The variables such as pyrocatechol and PEG 1500 ratio, stirring rate, stirring time, and solvent addition rate were operated through BBD to investigate their effect on solubility, drug release, and product yield. To optimize and achieve quality target product profile, the optimized batch was validated for getting a correlation between a theoretical value obtained from DoE and the practical value. The characterization parameters such as FT-IR, FT-^{1}HNMR, DSC, PXRD, and SEM indicated toward generation of different CUR crystals as that of unprocessed one.

Both crystals were further converted into tablet and tested for various quality control parameters. The results of the quality control parameters of the tablet were found well within the pharmacopeia limits. The dissolution studies revealed a significantly higher dissolution rate of optimized CUR crystals as that of the unprocessed form. Furthermore, the result of dissolution studies was well supported by *in vivo* pharmacokinetic study carried out on rats, in which oral bioavailability of optimized CUR crystals was found to be 7.08-folds greater than the unprocessed CUR crystals. The optimized CUR crystals were found stable at accelerated stability conditions for 6 months.

DISCLOSURE STATEMENT

No competing financial interests exist.

REFERENCES

1. Blagden N, de Matas M, Gavan PT, York P: Crystal engineering of active pharmaceutical ingredients to improve solubility and dissolution rates. *Adv Drug Deliv Rev* 2007;59:617–630.
2. Bhatt P, Lalani R, Vhora I, *et al.*: Liposomes encapsulating native and cyclodextrin enclosed paclitaxel: enhanced loading efficiency and its pharmacokinetic evaluation. *Int J Pharm* 2018;536:95–107.
3. Resnati G, Boldyreva E, Bombicz P, Kawano M: Supramolecular interactions in the solid state. *IUCrJ* 2015;2:675–690.
4. Kitamura M: Controlling factor of polymorphism in crystallization process. *J Cryst Growth* 2002;237:2205–2214.
5. Kitamura M: Controlling factors and mechanism of polymorphic crystallization. *Cryst Growth Des* 2004;4:1153–1159.
6. Bezerra MA, Santelli RE, Oliveira EP, Villar LS, Escaleira LA: Response surface methodology (RSM) as a tool for optimization in analytical chemistry. *Talanta* 2008;76:965–977.
7. Sanphui P, Goud NR, Khandavilli UR, Bhanoth S, Nangia A: New polymorphs of curcumin. *Chem Commun* 2011;47:5013–5015.

8. Fazel Nabavi S, Thiagarajan R, Rastrelli L, *et al.*: Curcumin: a natural product for diabetes and its complications. *Curr Top Med Chem* 2015;15:2445–2455.
9. Kumar B, Garg V, Singh S, *et al.*: Impact of spray drying over conventional surface adsorption technique for improvement in micromeritic and biopharmaceutical characteristics of self-nanoemulsifying powder loaded with two lipophilic as well as gastrointestinal labile drugs. *Powder Technol* 2018;326:425–442.
10. Carr RL: Evaluating flow properties of solids. *Chem Eng* 1965;18:163–168.
11. Elbary AA, Ali AA, Aboud HM: Enhanced dissolution of meloxicam from orodispersible tablets prepared by different methods. *Bull Fac Pharm Cairo Univ* 2012;50:89–97.
12. Patel J, Amrutiya J, Bhatt P, Javia A, Jain M, Misra A: Targeted delivery of monoclonal antibody conjugated docetaxel loaded PLGA nanoparticles into EGFR overexpressed lung tumour cells. *J Microencapsul* 2018;35:204–217.
13. Jangid NK, Chauhan NP, Ameta C, Meghwal K, Ameta R, Punjabi PB: Synthesis and characterization of functionalized polyaniline having methyl violet as pendant groups. *J Macromol Sci A* 2014;51:625–632.
14. Renuka S, Sachin Kumar, Gulati M, Kaur I: Characterization of solid state forms of glipizide. *Powder Technol* 2014;264:365–376.
15. Garg V, Kaur P, Singh SK, *et al.*: Solid self-nanoemulsifying drug delivery systems for oral delivery of polypeptide-k: formulation, optimization, in-vitro and in-vivo antidiabetic evaluation. *Eur J Pharm Sci* 2017;109:297–315.
16. Indian Pharmacopoeia: Uniformity of content of single-dose preparations. The Indian Pharmacopoeia Commission, Central Indian Pharmacopoeia Laboratory, Govt. of India, Ministry of Health & Family Welfare, Ghaziabad, 2008, p. 182.
17. Zade P, Kawtikwar P, Sakarkar D: Formulation, evaluation and optimization of fast dissolving tablet containing tizanidine hydrochloride. *Int J Pharm Tech Res* 2009;1:34–42.
18. Prudhviraj G, Vaidya Y, Singh SK, *et al.*: Effect of co-administration of probiotics with polysaccharide based colon targeted delivery systems to optimize site specific drug release. *Eur J Pharm Biopharm* 2015;97:164–172.
19. Singh SK, Yadav AK, Prudhviraj G, Gulati M, Kaur P, Vaidya Y: A novel dissolution method for evaluation of polysaccharide based colon specific delivery systems: a suitable alternative to animal sacrifice. *Eur J Pharm Sci* 2015;73:72–80.
20. Kumar B, Malik AH, Sharma P, *et al.*: Validated reversed-phase high-performance liquid chromatography method for simultaneous estimation of curcumin and duloxetine hydrochloride in tablet and self-nanoemulsifying drug delivery systems. *J Pharm Res* 2017;11:1166.
21. International Conference on Harmonization: Q2 (R1): Validation of analytical procedures: text and methodology. Paper presented at: International Conference on Harmonization, Geneva, 2005.
22. Shah VP, Tsong Y, Sathe P, Liu J-P: In vitro dissolution profile comparison—statistics and analysis of the similarity factor, f2. *Pharm Res* 1998;15:889–896.
23. Sanphui P, Goud NR, Khandavilli UR, Nangia A: Fast dissolving curcumin cocrystals. *Cryst Growth Des* 2011;11:4135–4145.
24. Orola L, Veidis MV, Sarcevica I, Actins A, Belyakov S, Platonenko A: The effect of pH on polymorph formation of the pharmaceutically active compound tianeptine. *Int J Pharm* 2012;432:50–56.
25. Thorat AA, Dalvi SV: Solid-state phase transformations and storage stability of curcumin polymorphs. *Cryst Growth Des* 2015;15:1757–1770.

Address correspondence to:
Sachin Kumar Singh, MPharm, PhD
School of Pharmaceutical Sciences
Lovely Professional University
Phagwara 144411
Punjab
India

E-mail: singhsachin23@gmail.com;
sachin_pharma06@yahoo.co.in

Abbreviations Used

β-CD = beta cyclodextrin
ANOVA = analysis of variance
API = active pharmaceutical ingredient
AUC = area under the curve
BBD = Box–Behnken design
BD = bulk density
CUR = curcumin
DMSO = dimethyl sulfoxide
DSC = diffraction scanning calorimetry
FT-^{1}HNMR = Fourier transform proton nuclear magnetic resonance
FT-IR = Fourier-transform infrared spectrophotometer
HPLC = high performance liquid chromatography
HR = Hausner ratio
LAP = liquid antisolvent precipitation
NMR = nuclear magnetic resonance
PEG = polyethylene glycol
PXRD = powder X-ray diffraction
QbD = quality by design
RH = relative humidity
SA = succinic acid
SD = standard deviation
SEM = scanning electron microscopy
TD = tapped density
WS = working standard